Extracellular Vesicles Enhance Osteogenic Differentiation of Mesenchymal Stem Cells without any Chemical Agents

Ganga Anand
Sree Chitra Tirunal Institute for Medical Sciences and Technology (SCTIMST)
Srinivas Gopala
Sree Chitra Tirunal Institute for Medical Sciences and Technology (SCTIMST), Medical College
Madhusoodanan Urulangodi
drmadhusoodanan@sctimst.ac.in
Sree Chitra Tirunal Institute for Medical Sciences and Technology (SCTIMST), Medical College
Manoj Komath
Sree Chitra Tirunal Institute for Medical Sciences and Technology (SCTIMST)

Research Article

Keywords: Extracellular Vesicles, Rat Bone Marrow Mesenchymal Stem Cells, Osteogenesis, Ultracentrifugation, Bone Regeneration

Posted Date: January 2nd, 2025

DOI: https://doi.org/10.21203/rs.3.rs-5741549/v1

Additional Declarations: No competing interests reported.

Abstract

The use of extracellular vesicles (EVs) in bone tissue engineering is emerging as a promising alternative strategy to stem cells. For clinical application, EVs must be biomanufactured from suitable source cells, systematically characterized, and validated for their efficacy in bone regeneration. This study focuses on the possibility of this translation using in vitro methods with rat bone marrow stem cells (rBMSCs). Bone marrow was harvested from Wistar rats and cultured using the direct adherence method. The rBMSCs were characterized through trilineage differentiation, flow cytometry, immunofluorescence, and real-time PCR. The optimal isolation method of EVs derived from the rBMSC was investigated. EVs isolated through ultracentrifugation yielded homogeneous EVs with good quality and quantity. The EVs derived from rBMSCs were characterized through Nanoparticle Tracking Analysis, Dynamic Light Scattering, Transmission Electron Microscopy, and Western Blot analysis. The osteogenic differentiation of rBMSCs was evaluated using the isolated EVs, confirmed by the MTT Cell Proliferation Assay and In vitro Osteogenesis Assays. The concentration- and time-dependent enhancement of osteogenic differentiation by rBMSC-derived EVs was also examined. Most importantly, EVs promoted osteogenic differentiation without adding any conventional chemical agents in the culture media. These findings will pave the way for further investigations to link EVs' therapeutic benefits in bone tissue engineering and related applications.

INTRODUCTION

Among the four main types of stem cells that are the candidates for bone tissue engineering (adult stem cells, embryonic stem cells, extra-embryonic stem cells, and induced pluripotent stem cells), adult stem cells are particularly notable for their remarkable ability to self-renew and expand. They demonstrate multipotency, possess anti-inflammatory and immunomodulatory properties, and can secrete factors that facilitate or enhance tissue regeneration [1, 2]. Among them, bone marrow-derived stem cells (BMSCs) are the prime choice because they are pluripotent and possess self-renewing capabilities with low immunogenicity. They serve as a crucial source of osteoblasts and are vital for bone tissue repair by containing and releasing trophic factors [1–3]. Bone regeneration involves recruiting mesenchymal stem cells (MSCs) to the injury site, which is then succeeded by cell proliferation, differentiation into osteoblasts, and intramembranous ossification. [4].

Increasing evidence suggests that the positive impact of mesenchymal stem cells (MSCs) on tissue repair is primarily due to their stimulation of tissue-resident receptor cells through paracrine signaling rather than through direct differentiation into parenchymal cells to mend or replace damaged tissue [5]. EVs derived from BMSCs demonstrate therapeutic effectiveness and functional characteristics akin to those originating BMSCs, allowing them to promote pro-regenerative effects comparable to stem cell therapy. These EVs encapsulate and concentrate bioactive molecules, facilitating their targeted delivery to damaged tissues and thereby promoting tissue repair and regeneration [6, 7].

EVs are nano-sized particles enclosed by a lipid bilayer released by different types of cells into the extracellular space, ranging from approximately 20 nm to > 10 microns in diameter, most under 200 nm [8]. Their composition includes a diverse array of lipids, proteins, and nucleic acids, reflecting the characteristics of their parent cells, including ceramides, sphingomyelin, tetraspanins, and various RNA species, such as mRNA and microRNA [9]. EVs play crucial roles in intercellular communication, tissue repair, and cancer progression, and they hold potential as biomarkers and therapeutic agents in clinical applications [10]. These vesicles can promote bone formation by delivering osteoinductive factors directly to the injury site. EVs have been shown to possess proangiogenic properties, promoting the formation of new blood vessels crucial for bone regeneration [11].

The rBMSCs can differentiate into multiple mesodermal derivatives, particularly osteogenic cells such as osteogenic progenitors, osteocytes, osteoblasts, and bone lining cells. They also can become adipogenic and chondrogenic cells, with their differentiation influenced by physiological requirements or pathological states [12]. The isolation of high-quality EVs presents several challenges related to their yield, purity, and specificity. The yield of EVs can be limited due to the small quantity naturally secreted by cells and the inefficiencies of current isolation methods [13]. Optimizing culture conditions and isolation protocols are essential for enhancing EV production. Contaminants such as proteins, lipids, and other particles often co-isolate with EVs, compromising their purity and functionality. Removing these contaminants without significantly losing EVs remains a major challenge [14]. Techniques like ultracentrifugation, density gradient centrifugation, and other popular methods can result in contamination from non-EV particles and protein aggregates. These methods also require long processing times and specialized equipment [15, 16]. Precipitation methods, including those using commercial kits, can lead to high levels of protein contamination and variability in yield [13, 17].

This study seeks to investigate three important components of EVs in the context of regenerative medicine. First, it seeks to identify the optimal source cells for the production of EVs, ensuring that the most effective cellular origins are utilized. Second, the study focuses on refining EV isolation techniques to enhance the purity and functionality of the isolated vesicles. Finally, it aims to evaluate the ability of these isolated EVs to promote osteogenic differentiation in progenitor cells. By focusing on these objectives, the study aims to provide important insights into the significance of EVs in bone tissue engineering and regenerative therapies.

MATERIALS AND METHODS

Isolation, Expansion, and Characterization of rBMSCs

Bone marrow was harvested from four-week-old Wistar rats following approval from the Institutional Animal Ethics Committee (IAEC) of SCTIMST (SCT/IAEC/TR-02/116/AUG/2023). Bone marrow was collected and processed from femurs and tibias of rat according to the standard protocol [18]. Two methods were used to extract rat bone marrow stem cells (rBMSCs): direct adherence and density gradient centrifugation. For the direct adherence method, MSCs were isolated based on their ability to

adhere to tissue culture plates, according to the previously established protocol [19]. MSCs were subcultured using a 0.25% trypsin-0.53 mM EDTA solution (Sigma #85450C, US; Merck #108421, US). The cells were then centrifuged, resuspended in complete medium, and transferred to a T75 flask to establish passage one (P_1). This subculturing process continued until P_3 with a split ratio of 1:3. Bone marrow cell suspension was carefully placed on top of an equal volume of HiSep (Himedia #LS001, India) and processed as described for density gradient isolation [20]. Cell cultures were routinely checked for confluence, morphology, and phenotypic characteristics using an inverted fluorescence and phase-contrast microscope (Olympus IX51, Japan).

Characterization of rBMSC

Trilineage Differentiation

To assess the multi-lineage differentiation potential of the isolated rBMSCs, differentiated them into osteogenic, adipogenic, and chondrogenic lineage using respective standard induction media [21]. The media was changed at 3-day intervals for 21 days. Osteogenic, chondrogenic, and adipogenic differentiation were confirmed by Alizarin Red S, Alcian blue, and Oil Red O staining, respectively; images were captured using an inverted fluorescence and phase contrast microscope (Olympus IX51, Japan).

Immunofluorescence staining and flow cytometry analysis of rBMSCs: MSCs were characterized for the presence of specific cell surface markers using standard protocol [22] with specific primary antibodies (1:100), Thy1/CD90 (Invitrogen #MA1-81491), Endoglin/CD105 (NeoBiotechnologies #2022-MSM6), and CD34 (NeoBiotechnologies #947-MSM1). Goat anti-mouse 488 secondary antibody (Abcam, #ab150117) at a dilution of 1:200 was used according to the manufacturer's instructions, samples were mounted with an anti-fading medium DAPI (G-Biosciences #IHS2110A, USA) and examined under an inverted fluorescence microscope (Axio Observer, Carl Zeiss Microscopy, Germany).

To assess the homogeneity of rBMSCs, cells were analyzed by flow cytometry with primary antibodies against CD90, CD105, and CD34. Analysis was performed using a FlowSight system, with data processed using IDEAS software. (Amnis, part of EMD Millipore, Seattle, WA, USA).

Quantitative Real Time-PCR

Total RNA was extracted from cells using using traditional TRIzol method (TRI reagent, Sigma #T942, US), and RNA quality and purity were evaluated using a NanoDrop spectrophotometer. (Nanodrop One; Thermo Fisher Scientific, USA). According to the manufacturer's instructions, the cDNA was synthesized with PrimeScript 1st strand cDNA Synthesis Kit (TaKaRa #6110A, Japan). Expression levels were normalized to β-Actin. PCR was performed for positive markers (CD73, CD90, and CD105) and negative marker (CD34) in RT-PCR system (Bio-Rad CFX96, Real-time system, C1000 Touch, Singapore).

Isolation of rBMSC-derived EVs

rBMSCs were seeded in 100 mm culture dishes at 10000 cells/cm^2 density and maintained under standard conditions until they reached 70%-80% confluence. Subsequently, the growth medium was removed and replaced with 10 ml of serum-free DMEM-LG medium. The cells were then incubated under standard conditions for 48 h, the supernatant from the cell culture was harvested for isolating EVs. To determine the optimal isolation method, 30 ml of collected media was divided and subjected to the following three protocols:

Total Exosome Isolation (TEI) reagent: 10 ml of cell culture supernatant underwent centrifugation at 2000 × g for 10 min at 4°C. The resulting supernatant was combined with TEI reagent (#4478359; Invitrogen, USA) in a 2:1 volume ratio. This mixture was incubated overnight at 4°C, then centrifuged at 10,000 × g for 1 h at 4°C [23]. EV containing pellet was resuspended in 50µl of ice-cold 1X PBS and kept at -80°C for subsequent analysis.

Polyethylene Glycol (PEG) Precipitation

Cell culture supernatant (10 mL) was centrifuged at 2000 × g for 10 min at 4°C. An equivalent volume of 2X PEG stock solution (PEG 8000 Sigma #P2139, Germany) was combined with the supernatant obtained. The mixture was then incubated overnight at 4°C, followed by centrifugation at 10,000 × g for one hour at 4°C [24]. The EV pellet obtained was resuspended in 50 µl of ice-cold 1X PBS and kept at -80°C for subsequent analysis.

Ultracentrifugation (UC)

10 ml of cell culture supernatant was centrifuged at 300 x g for 10 min, 2000 x g for 10 min, 10000 x g for 40 min at 4°C to eliminate dead cells, microvesicles, apoptotic bodies, and cellular debris. The cleared supernatant was transferred to ultracentrifuge tubes and spun at 100000 x g for 70 min at 4°C using a Himac CS150 GXII micro-ultracentrifuge (HITACHI Koki Co. Ltd., Japan) with a type S80AT3-2062 rotor. EV pellet was resuspended in 1ml of ice-cold 1X PBS, pooled, and subjected to another centrifugation at 100000 x g for 70 min at 4°C [25]. The final EV pellet was resuspended in 50µl of ice-cold 1X PBS and stored at -80°C for future analysis.

Characterization of EVs

Transmission Electron Microscopy (TEM)

For TEM analysis, the EV samples were fixed with 100 µl of 1% glutaraldehyde in PBS [26]. The sample was then dropped onto Formvar-coated EM grids and dried overnight. It was then stained with UranyLess stain (EM Sciences, USA), air-dried, and visualized at 80KV using TEM (Hitachi H-7650, Japan).

Dynamic Light Scattering (DLS) Analysis: Zetasizer (Nano series Nano-ZS ZEN3600, Malvern Panalytical Instruments, US) was employed to examine the size distribution of EVs obtained from rBMSCs. The EV suspension was diluted 1:100 with molecular-grade water for analysis. Intensity plots were used to

graphically illustrate the size distribution of EVs from various isolates, with measurements conducted in triplicate.

Nanoparticle Tracking Analysis (NTA): Particle number and size of rBMSC-derived EVs were determined using NTA. The zeta view particle tracking analyzer (Particle Metrix, Laser scattering video microscope, Germany) performed NTA. The samples were diluted 1:100 in ultrapure water and analyzed as previously described [27].

Total protein estimation, SDS-PAGE, and Western Blot Analysis: The BCA assay kit (G-Biosciences #786–844, India) was employed to determine the total protein content of EVs, following the manufacturer's instructions. Proteins were resolved using denaturing SDS-PAGE and transferring onto PVDF membrane (Merck, Millipore, US, #IPVH00010). Primary antibodies against TSG101 (1:2000, Puregene #PG-80736), HSP90 (1:1000, Cell Signaling Technology #8165S), and CD9 (1:1000, Cell Signaling Technology #13403S). The signal was detected using a gel documentation system (G-Box ChemiXRQ, Syngene, UK).

Preparation of EV-depleted FBS (ED-FBS) and Enhanced Cell Culture Scalability

Centrifugation steps were used to extract bovine EVs from FBS and create EV-depleted FBS for isolating rBMSC-derived EVs. The process began with undiluted FBS or a 1:3 mixture of FBS and cell culture media. These samples underwent centrifugation at 2000 × g for 10 min, 10,000 x g for 40 min at 4°C to eliminate cell debris and larger particles [28, 29]. The supernatant was transferred to ultracentrifuge tubes and ultracentrifuged at 120,000 × g at 4°C for 2 h using a Himac CS150GXII (HITACHI Koki Co. Ltd, Japan) with a type S80AT3-2062 rotor. The final supernatant, now ED-FBS, was filtered through 0.22 µm syringe filters and stored at -20°C. The pellet, potentially containing FBS-EVs, was resuspended in 250 µl of 1X PBS and kept at -80°C. Coomassie staining and western blot analysis were performed with exosomal markers to evaluate the depletion process and confirm the depletion method's effectiveness.

To increase EV yield, rBMSCs cultures were expanded to T150 flasks. The cells were initially grown in T25 or T75 flasks until reaching P_3. P_3 cells were then trypsinized and seeded into T150 flasks at a density of 10×10^5 cells each, cultured in complete media. Upon reaching 70–80% confluency, the medium was replaced with 20 ml of DMEM-LG supplemented with 10% ED-FBS. After a 48-hour incubation period for EV secretion, the supernatant was collected and subjected to differential ultracentrifugation for EV isolation as previously mentioned. The size of the EVs was validated using NTA and DLS, followed by total protein estimation, SDS-PAGE and western blot analysis to identify exosomal markers.

Osteogenic differentiation in the presence of EVs

MTT Cell Proliferation Assay

A total of 5×10^3 cells/cm^2 were seeded in a 24-well plate and cultured in complete media. After 24h, cells were treated in triplicates with 0, 10, 20, 40 and 60 µg/mL rBMSC-derived EVs weekly twice for 14 days, MTT assay was used to investigate cell proliferation. After removing the medium, the cells were washed with PBS and treated with 500 µL/well of 3-(4,5-dimethylthiazolyl2)-2,5-diphenyltetrazolium bromide (1µg/mL MTT in PBS, Sigma, USA). The purple MTT formazan crystals were dissolved in DMSO and absorbance was measured at 570 nm.

Based on the cell viability assay, the experimental setup comprised two primary treatment groups: Differentiation Media (DM) and Complete Media (CM). Each group was subdivided based on the concentrations of rBMSC-derived EVs supplemented, specifically 12.5 µg/ml and 25 µg/ml. Additionally, the CM group included three higher concentrations of EVs (50, 75, and 100 µg/ml).

In vitro Osteogenesis Assays

To assess the osteogenic differentiation capacity of MSCs enhanced with EVs, cells were grown under various experimental conditions. The cultures were sustained for 7, 14, 21, and 28 days, after which they were treated with 40 mM ARS, following established protocols, and examined using an inverted microscope.

qRT-PCR was employed to measure osteogenic gene expression. The expression levels of specific osteogenic *genes (ONC, OPN, RUNX2, BMP2, BMP4, OSX, OCN, ALP*, and *COL1α1)* were evaluated as previously described, with normalization to an internal β-Actin. The data was analyzed using the comparative threshold cycle (ΔΔCT) approach and presented as relative mRNA expression levels.

Protein extraction was performed using RIPA buffer (Merck Millipore, #20–188, USA), and total protein content was determined on days 7, 14, 21, and 28 of rBMSC culture utilizing the BCA Protein Assay. Western blot analysis was conducted, using specific primary antibodies: Anti-RUNX2 (1:1000, Goat Anti-Rabbit IgG, Cell Signaling Technology), Anti-COL1α1 (1:1000, Goat Anti-Mouse IgG, Abcam), and Anti-GAPDH Rabbit mAb (1:1000, #2118, Cell Signaling Technology, USA). The protein bands were quantified using ImageJ software.

Statistical analysis

Each experiment was conducted using a minimum of three separate samples. Results are expressed as mean ± SD (standard deviation). Statistical analysis was performed using GraphPad Prism 10 software, with significance set at $P < 0.05$. T-tests were employed to assess statistical differences. Representative figures were generated using Biorender software (https://biorender.com/).

RESULTS

Characterization of homogeneous rBMSCs derived through optimized Direct Adherence method

To determine the optimal isolation method for obtaining rBMSCs from rat bone marrow, we compared two commonly used techniques: direct adherence and density gradient centrifugation (**Fig. S1a**). The ability of rBMSC to adhere to the culture dish was tested for culture expansion. We observed comparable rounded cell morphology at early time points for both methods. However, direct adherence resulted in higher cell density than density gradient centrifugation-based isolation. Cells consistently adhered after three days, with more cells in the direct adherence method. The direct adherence method resulted in a progressive change in morphology from rounded to spindle in most cells, whereas density gradient centrifugation resulted in a few cells reaching spindle morphology. Cells isolated by direct adherence became 70–80% confluent after 5 days and were subcultured with 0.25% trypsin-EDTA solution (**Fig. S1b**), whereas the cells isolated by density gradient centrifugation were degenerated (**Fig. S1c**). After three passages, a homogeneous fibroblastic cell monolayer was formed in cells cultured by direct adherence isolation, reaching confluence within 4–5 days. It is important to note that washing the cells with DPBS is crucial to remove cellular secretions and residual medium and loosen up the adhesive force of MSC in the culture flasks. Trypsin digestion should be limited to 2 min because prolonged digestion would detach non-MSCs from the culture flask and be detrimental to MSCs. rBMSCs isolated from young animals, specifically those younger than three months old, exhibited notably higher cell viability than rBMSCs isolated from animals older than three months. When subjected to specific in vitro conditions and exposed to lineage-specific differentiation media for 4 weeks, the MSCs obtained through direct adherence successfully transformed into adipocytes, osteocytes, and chondrocytes. Adipose-differentiated MSCs exhibited intracellular lipid droplets, verified using Oil Red O staining (**Fig. S1d**). Cells that differentiated into osteocytes formed mineralized nodules, identified positively by ARS staining (**Fig. S1e**). MSCs induced with chondrogenic medium produced sulfated proteoglycans and glycosaminoglycans, which were visualized using Alcian Blue staining (**Fig. S1f**). Undifferentiated cells from all experimental groups showed no such staining.

Subsequently, MSC-specific markers were assessed through immunocytochemical staining. The cells exhibited positive results for MSC-specific surface markers CD90 and CD105 while showing negative results for CD34 (**Fig. S2a**). Flow cytometry analysis revealed that over 97% of the cells were positive for CD90 (**Fig. S2b**) and more than 99% for CD105 (**Fig. S2c**), with less than 1% showing positivity for the negative marker CD34 (**Fig. S2d**). Images of the cells analyzed by flow cytometry were captured and displayed below each figure. Additionally, qRT-PCR analysis of cell surface antigens indicated a uniform population of differentiated MSCs. rBMSCs isolated using the direct adherence method expressed the positive markers CD73, CD90, and CD105. In contrast, the negative marker CD34 was not detected (**Fig. S2e**). These findings demonstrated that the cells isolated and cultured via the direct adherence method were homogeneous and mesenchymal in nature. As a result, the direct adherence method was utilized in subsequent experiments.

Isolation of extracellular vesicles with high purity and yield by Ultracentrifugation

To determine the most effective technique for isolating EVs, we evaluated the efficiency of three commonly used methods: Total Exosome Isolation Kit (TEI), polyethylene glycol (PEG) precipitation, and ultracentrifugation (UC). Cell culture supernatants from rBMCs cultured using the direct adherence method were used for this assessment (Fig. 1a). To evaluate the size distribution, freshly isolated EVs were subjected to DLS measurements. The results revealed that all EV preparations, except those isolated using the TEI kit, were within the expected size range of approximately 200 nm. Specifically, EVs isolated with the TEI kit exhibited a broader size distribution, with a prominent intensity peak at 2757 ± 21.5 nm and a weaker intensity peak at 70.83 ± 4.7 nm. In contrast, EVs isolated by UC had an average size of 210.8 ± 19.94 nm, while those obtained via the PEG precipitation method averaged 181.7 ± 15.68 nm (Fig. 1b). These findings suggest that both the UC and PEG precipitation methods effectively yield a homogeneous mixture of EVs within the anticipated size range. This finding also highlights the importance of choosing appropriate isolation techniques for obtaining high-quality EV preparations for downstream applications.

To further compare the efficacy of the different EV isolation methods, the total EV yield was quantified by measuring protein concentration using the BCA assay kit. Results indicated that the UC method produced the highest protein yield, followed by the PEG precipitation method, while the TEI kit method yielded the least amount of protein (Fig. 1c). The efficiency of EV isolation was further evaluated using SDS-PAGE followed by Western blot analysis. Coomassie staining of SDS-PAGE gels revealed much higher protein bands in EVs isolated via the UC method (Fig. 1d). Additionally, Western blot analysis demonstrated the presence of EV markers, such as CD9 and TSG101 in EVs isolated by both the UC and PEG methods, but not in those isolated using the TEI kit (Fig. 1E). From 10 ml of rBMSC culture supernatant, the UC method yielded the highest protein concentration, making it the preferred method for subsequent experiments. However, it is important to note that while the UC method provided the maximum yield, the protein concentration obtained might still be insufficient for further downstream applications like osteogenic differentiation experiments. This limitation underscores the need to optimize EV isolation protocols or explore alternative methods to achieve higher yields suitable for advanced experimental requirements.

Enhanced Yield of Extracellular Vesicles in rBMSC Cultures through Culture Expansion and ED-FBS

To maximize the yield and quality of EVs from rBMSC cultures, the culture conditions were optimized by combining a scale-up approach with the use of EV-depleted FBS (ED-FBS). This strategy addresses two critical aspects: minimizing the presence of bovine EVs in standard FBS, which can interfere with the purity and specificity of isolated EVs, and increasing the overall cell number to enhance EV production (Fig. 2a). To assess the effectiveness of EV depletion from FBS, Coomassie staining was performed on both ED-FBS and the EV pellet obtained after ultracentrifugation of FBS (FBS-EV) samples prepared using two different methods: undiluted or diluted with cell culture media at a 1:3 ratio (FBS: culture media). The staining revealed depletion of protein bands corresponding to EV proteins in ED-FBS samples, whereas these bands were present in FBS-EV fractions prepared by both methods. This

indicates the successful removal of EVs from FBS (**Fig. S3a**). Additionally, Western blot analysis using EV markers was performed to validate the depletion process. HSP90 and TSG101 were not detected in ED-FBS, whereas they were present in the EV samples isolated using corresponding methods (**Fig. S3b).** These findings confirm successful EV depletion, ensuring that the supernatant is free of EVs from FBS.The scale-up process involved increasing the cell number by expanding rBMSC cultures from smaller T25 flasks to larger T150 flasks. This scaling up of culture volume is expected to increase the number of cells, thereby enhancing the potential yield of EVs. Isolated EVs were subjected to dynamic light scattering (DLS) analysis. The size measurement showed that EVs from both conditioned media groups (ED-FBS and serum-free) were approximately 200 nm in diameter after the scale-up process with 100% intensity peaks. EVs derived from serum-free media showed a prominent intensity peak at 203 ± 23 nm, while EVs isolated from ED-FBS supplemented media had an average size of 157 ± 20 nm (**Fig. S3c**).

We compared the protein concentration of EVs isolated after scaling up the process with ED-FBS supplementation to those isolated from serum-free cell culture supernatants. The results showed a significant increase in yield for EVs from scaled-up cell culture supernatants. Additionally, EVs from cell culture supernatants supplemented with ED-FBS had an even greater yield compared to those from serum-free media (Fig. 2b). Increased protein concentrations were also apparent in the SDS-PAGE analysis (Fig. 2c). Furthermore, Western blot analysis indicated increased expression of exosomal markers CD9, TSG101, and HSP90 in the EVs isolated by combining the scale-up process with ED-FBS supplementation (Fig. 2d).

The EVs isolated from ED-FBS supplemented media were analyzed for size distribution and morphology using NTA and TEM, respectively. A three-dimensional plot of relative intensity was used to represent NTA data. The concentration of EVs was 3.3×10^6 particles/ml, with a mean diameter of 96.6 ± 56.1 nm (Fig. 2e). This shows that scaling up rBMSC cultures and using ED-FBS was an effective approach for obtaining a high quantity and purity of EVs for downstream applications. TEM data revealed typical EV appearance with diameters within the 200 nm range (Fig. 2f). Thus, using ED-FBS ensures the isolation of EVs from rBMSC cultures devoid of FBS-EV contaminants while still providing essential growth factors and nutrients. This approach maintains superior cell viability and functionality compared to serum-free conditions, enhancing EV production. As a result, we have adopted this protocol for our subsequent experiments.

Osteogenic differentiation dynamics in rBMSCs

The differentiation of rBMSCs into osteogenic lineage was induced over a period of 7, 14, 21, and 28 days (**Fig. S4a**). Compared to the control group, rBMSCs undergoing in vitro osteogenic differentiation showed rapid proliferation, forming tightly packed colonies. These colonies developed dense, granular areas, and after two weeks of culture, multiple cell layers often appeared, sometimes leading to cell death due to prolonged osteogenic treatment.

To assess osteogenic differentiation, we stained monolayers with Alizarin Red at various time intervals to measure calcium deposition. The results revealed that exposure to an osteogenic medium led to the

significant formation of mineralized nodules over time. Specifically, intense positive staining was observed at later stages (days 21 and 28), with lower levels seen at earlier stages (days 7 and 14). In contrast, the control samples showed no calcium mineralization throughout the duration. These findings indicated a progressive increase in mineralization correlating with the duration of osteogenic induction (**Fig. S4b**).

Osteogenic differentiation was evaluated by quantifying the expression of various markers, including *ONC, OPN, RUNX2, β-actin, OSX, OCN, COL1α1, BMP2, BMP4* and *ALP*, using qRT-PCR. The primary molecular regulator RUNX2 plays a crucial role in directing the differentiation of MSCs into preosteoblasts. RUNX2 is expressed early in differentiation to promote osteogenesis while inhibiting adipogenesis and chondrogenesis. It regulates numerous downstream osteogenic genes, such as *OSX, OCN, ALP, ONC, OP*, and *COL1α1* [30]. Increased expression of *RUNX2* mRNA was observed in the early stages of differentiation starting from day 7, followed by a decline in the late stage (day 28), consistent with previous reports [31]. *OSX* expression was upregulated during the early differentiation stage, progressively increasing over time. MSCs exhibited elevated *OPN* mRNA transcript levels during the late stages of differentiation (days 21 and 28). Additionally, ONC, BMP2, COL1α1, ALP, and BMP4 mRNA transcripts were highly expressed at days 14 and 21 (**Fig. S4c**).

We investigated osteogenesis by examining the expression of specific osteogenic proteins using immunofluorescence. Expression of RUNX2 and COL1α1 proteins were evaluated in rBMSCs cultured in osteogenic medium for 7, 14, 21, and 28 days. The results showed that both RUNX2 expressions were significantly higher in the day 7 and 14 groups compared to the later stages of differentiation. The expression of COL1α1 was consistent at all four time points (**Fig. S4d**).

Concentration and time-dependent enhancement of osteogenic differentiation by rBMSC-derived EVs

To assess the potential of EVs to enhance cell proliferation, varying concentrations (0, 10, 20, 40, and 60μg/ml) of EVs were incubated with rBMSCs for 14 days. MTT assay results revealed a concentration-dependent increase in cellular proliferation with higher concentrations of EVs (Fig. 3a). Importantly, no cytotoxic effects were observed across any concentration, highlighting the safety and efficacy of rBMSC-derived EVs in promoting cell proliferation. The ability of rBMSC-derived EVs to enhance osteogenic differentiation was evaluated by two different concentrations of EVs (12.5 and 25μg) in the presence and absence of osteogenic stimulants (Fig. 3b).

The deposition of calcium, leading to bone mineralization, is considered a late indicator in the osteogenic differentiation process [32]. ARS staining results demonstrated that EVs from rBMSCs significantly enhanced osteogenic differentiation depending on both concentration and treatment duration. Examination of mineralization scans revealed that EV supplementation induced calcium deposition in both CM and DM groups. These groups showed increased mineralization, evidenced by darker staining, coarser particles, and more extensive branched deposits than the untreated group. The most significant differences in mineralization were evident after 14 days in the EV-treated groups. EV

administration in the DM treatment group resulted in a concentration and time-dependent increase (Fig. 3c). Notably, in the CM group lacking osteogenic reagents, EVs induced mineralization, suggesting that rBMSC-derived EVs possess inherent osteogenic capabilities. The CM + 25µg EVs exhibited considerable calcium deposition compared to the CM + 12.5µg EVs. While no distinct mineral deposits were visible until day 14, faint, weakly stained mineral particles appeared on day 21. They increased further by day 28 of treatment (Fig. 3d). Both image analysis and quantification of extracted ARS stain indicated a significant increase in mineralization in the EV-treated groups compared to the untreated group on days 7, 14, 21, and 28 (**Fig. S5a-S5b**).

Next, qRT-PCR evaluated the expression of osteogenic markers in rBMSCs treated with EVs under both CM and DM conditions. The analysis showed a consistent trend in the expression of key osteogenic markers across different time points, underscoring the osteogenic potential of rBMSC-derived EVs. Osteoblasts differentiate from their precursors through the modulation of several transcription factors during osteogenesis, including the master transcription factor *RUNX-2* and its downstream target *OSX* [31]. These transcription factors are crucial in the cell-fate decision process that drives MSCs to become osteoblasts. In the DM group, *RUNX2* expression levels increased seven-fold in the DM + 25µg EVs. In contrast, *OSX* expression significantly increased from day 7 to day 14 in the same group, showing a 26-fold increase, indicating early osteogenic differentiation (Fig. 4a). From day 21 onwards, there was a gradual decline in the expression of these markers, suggesting peak activity during the initial differentiation phase. *RUNX2* and OSX, together, are responsible for expressing osteoblast proteins, including other early osteogenic markers such as *ALP, COL1α1*, and various non-collagenous proteins. Early osteogenic markers like *BMP2, BMP4, COL1α1, ALP*, and *ONC* showed marked increases in expression, with 59-fold, 10-fold, 13.5-fold, 46-fold, and 7-fold changes respectively during days 14 and 21 (Fig. 4a**).** *BMP2 and BMP4*, which are critical for osteoblast differentiation, along with *COL1α1, ALP, and ONC*, exhibited elevated levels, highlighting their roles in extracellular matrix formation and mineralization processes. Late osteogenic markers *OCN and OPN* showed a 29.5-fold increase from day 7, peaking at day 28, correlating with advanced stages of bone matrix maturation and mineralization (Fig. 4a).

Notably, the CM + 25µg EVs also demonstrated consistent increases in the expression levels of osteogenic markers across all time points compared to other treatment groups and controls (Fig. 4B). However, these increases were notably less pronounced than those observed in the corresponding DM-treated group. Similarly, CM without EV supplementation showed minimal osteogenic marker expression, highlighting the essential role of EVs in enhancing osteogenesis. In CM supplemented with 25 µg EVs, early osteogenic markers *RUNX2 and OSX* showed seven-fold and 238-fold increases, respectively. Along with *RUNX2 and OSX*, other early osteogenic markers such as *ONC, BMP2, and COL1α1* exhibited 21-fold, 54-fold, and 14-fold increases, respectively, at day 21. The CM + 12.5µg EVs also demonstrated significant increases in fold changes compared to the untreated group.

Additionally, protein expression levels of RUNX2 and COL1A1, were examined in rBMSCs exposed to EVs under both CM and DM conditions using western blot analysis. The expression of RUNX2 showed a

gradual increase from day 7 to day 14 in both CM and DM groups (Fig. 5a**).** This correlates with the qRT-PCR data, indicating that the early phase of osteogenic differentiation involves upregulation of RUNX2. By day 21, the expression of RUNX2 started to decline, aligning with the observed decrease in mRNA levels from qRT-PCR results. COL1A1 expression increased from day 7 to day 21, reflecting its role in forming the extracellular matrix during osteogenesis (Fig. 5b). DM alone induced RUNX2 and COL1A1 expression but at significantly lower levels than EV-treated groups. CM without EV supplementation showed minimal expression of these markers, underscoring the critical role of EVs in promoting osteogenic differentiation.

EVs enhance osteogenic differentiation without relying on conventional external chemical agents

Typically, osteogenic differentiation media includes L-ascorbic acid, dexamethasone, and β-glycerophosphate. However, it was observed that adding specific concentrations of EVs to complete media without these chemical differentiation agents induced rBMSC differentiation (Fig. 6c-d, S5b, 4b, and 5a-5b). We used FBS-EVs as a control to validate that this effect was specifically due to the rBMSC-derived EVs. We compared the osteogenic differentiation effects of EVs from rBMSCs to those from FBS. For 14 days, the complete media was supplemented with EVs from two different sources at varying concentrations (12.5, 25, 50, 75, and 100 µg/ml). ARS staining revealed that media supplemented with EVs promoted calcium deposition in a concentration-dependent manner even without osteogenic chemical stimuli (Fig. 6a). Notably, groups treated with rBMSC-derived EVs showed significantly higher calcium deposition levels compared to those treated with FBS-EVs (Fig. 6b). Extended exposure to rBMSC-derived EVs resulted in increased calcium deposition over time. Specifically, lower concentrations (12.5, 25, and 50 µg/ml) of rBMSC-derived EVs resulted in minimal calcium deposits, significantly increasing at higher concentrations (75 and 100 µg/ml). This suggests that rBMSC-derived EVs possess inherent osteogenic potential, with higher concentrations leading to more significant calcium deposition. Conversely, EVs derived from FBS demonstrated only a slight increase in calcium deposition at the given concentrations, less pronounced compared to the groups treated with rBMSC-derived EVs (Fig. 6c). To assess the protein expression levels of RUNX2, western blot analysis was conducted. The cells treated with rBMSC-derived EVS showed increased RUNX2 expression compared to the group treated with FBS-EVs (Fig. 6d). These results suggest that rBMSC-derived EVs are more effective in committing cells to the osteogenic lineage than FBS-EVs. Our findings indicate that rBMSC-derived EVs specifically induce osteogenic commitment in cells compared to FBS-EVs, suggesting the presence of distinctive signaling molecules within the EVs.

DISCUSSION

This study optimized the isolation and culture conditions for rBMSCs, and various techniques for isolating EVs were evaluated. The comparison between the direct adherence method and density gradient centrifugation for rBMSC isolation revealed results consistent with previous findings [17], the direct adherence method yielded a higher cell density and superior morphological progression, with cells

transitioning from a rounded to spindle shape within five days. This method produced a homogeneous fibroblastic cell monolayer after three passages and showed better cell viability and proliferative capacity, especially in rBMSCs isolated from younger animals. This aligns with previous studies indicating an age-related decline in stem cell functionality and viability [33, 34]. The isolated rBMSCs effectively differentiated into adipocytes, osteocytes, and chondrocytes under specific conditions, confirmed by trilineage differentiation assays, flow cytometry, immunofluorescence, and qRT-PCR analysis. The direct adherence method showed simple, higher MSC yield, improved cell purity, and better adherence and expansion capabilities, make it a preferred and reliable technique for isolating rBMSCs, essential for downstream applications and differentiation experiments [4, 35].

The next step was determining the most effective EV isolation method from rBMSCs, comparing UC, PEG precipitation, and the TEI kit. DLS analysis showed that EVs isolated by UC and PEG precipitation fell within the expected size range (~ 200 nm), while the TEI kit yielded a broader size distribution, as previously reported [36]. UC outperformed the other methods, achieving the highest protein concentration and EV purity, consistent with other studies showing UC's superior ability to isolate EVs with fewer contaminants. A recent study comparing the isolation techniques for small extracellular vesicles (sEVs) in breast cancer liquid biopsies revealed that UC yielded superior sEV purity, marker expression, and a higher quantity of sEV proteins compared to TEI and a combined approach [37]. Although PEG precipitation was effective, it did not match the yield and purity levels achieved by UC. In contrast, the TEI kit's broader size distribution and lower protein concentration suggested it may be unsuitable for high-purity EV applications. While UC is time-consuming and requires specialized equipment, its ability to produce high-quality EVs makes it preferable for applications such as clinical diagnostics and therapeutic use [35, 37]. Our findings underscore the effectiveness of the direct adherence method for rBMSC isolation and confirm UC as the optimal technique for EV isolation, providing a strong foundation for refining protocols to meet the stringent requirements of advanced research applications.

However, challenges remain regarding their mass production, separation efficiency, and characterization for clinical applications [6, 7]. Various innovative approaches have been explored to enhance EV yield, including physical and chemical stimulations, 3D bioreactor systems, and cell spheres, which have shown promise in increasing EV production [38–41]. However, these methods may cause cell stress or damage, potentially affecting EV integrity and functionality[37, 42]. Moreover, they are often complex and costly, limiting their routine use. Enhancing the yield of EVs and improving their storage stability remain significant challenges in assessing their potential for bone regeneration, both in vitro and in preclinical models. Adjusting cell seeding density and increasing the frequency of media collection effectively boosts EV production by reducing cell stress and preventing the accumulation of inhibitory factors [25, 41]. Additionally, using ED-FBS instead of serum-free media supports cell growth and minimizes contamination from bovine EVs [28, 43–44]. Our results demonstrated that supplementing cultures with ED-FBS increased EV yield, as evidenced by higher protein concentrations and enhanced EV marker expression (CD9, TSG101, HSP90) in Western blot analysis. The EVs displayed typical size distributions and morphology, suggesting that ED-FBS may influence vesicle populations or maturation states. This

strategy, combining scaled-up cell cultures and ED-FBS supplementation, supports large-scale EV isolation without compromising cell function or EV yield. These findings facilitated the successful implementation of a standardized protocol, allowing us to explore its potential for inducing osteogenic differentiation of rBMSCs under laboratory conditions.

In vitro, osteogenic differentiation in rBMSCs was assessed through morphological, biochemical, molecular, and protein expression analyses. rBMSCs cultured in osteogenic induction media containing dexamethasone, β-glycerophosphate, and L-ascorbic acid demonstrated rapid proliferation, forming densely packed colonies that developed mineralized nodules, as indicated by ARS staining, particularly at later stages (days 21 and 28). Molecular analysis through qRT-PCR revealed key osteogenic markers, with *RUNX2* peaking at days 14 and 21, signifying its role in osteogenesis. *OSX* expression increased throughout differentiation, indicating osteoblast maturation, while elevated *OPN* levels at days 21 and 28 marked ongoing matrix maturation. The expression patterns of *BMP2* and *BMP4* correlated with observed mineralization. *RUNX2* and *OSX* regulated osteoblast-specific proteins' expression, including *ALP* and *COL1a1*. *ALP* peaked at day 14, indicating early differentiation, while *OCN*, vital for bone matrix synthesis, peaked at day 21. Immunofluorescence confirmed *RUNX2* as an early osteogenic regulator, with *COL1a1* levels remaining high, suggesting continuous collagen production. These findings show how osteogenic differentiation is regulated over time in rBMSCs.

To determine the role of EVs, the study investigated the effect of supplementing rBMSC-derived EVs on osteogenic differentiation. The results demonstrated that these EVs significantly enhance the osteogenic differentiation of rBMSCs. EVs have been observed to stimulate the proliferation of recipient rBMSCs in a concentration-dependent manner while exhibiting no cytotoxic effects [28, 45–47]. Using the MTT assay, we also observed a concentration-dependent increase in cell proliferation with higher concentrations of EVs and no cytotoxic effects over 14 days. This indicates that rBMSC-derived EVs support cell viability and actively promote proliferation, providing a strong foundation for their use in regenerative medicine. Calcium deposition, an indicator of osteogenic differentiation, was evaluated using ARS staining. Previous studies demonstrated that EVs derived from human BMSCs (hBMSCs) at various stages of osteogenic differentiation significantly increased calcium deposition compared to controls [49]. Our study demonstrated that supplementing with EVs resulted in a concentration-dependent increase in mineralization in rBMSCs. The most significant mineralization was observed in the DM group treated with 25 μg/mL of EVs, with substantial calcium deposition evident by day 14 and further increased by days 21 and 28. EV supplementation also promoted osteogenic differentiation in the CM group, which lacked traditional osteogenic stimulants. This enhancement highlights the intrinsic osteogenic potential of rBMSC-derived EVs.

The expression of osteogenic markers at different time points was examined by qRT-PCR included markers for osteoprogenitors (*RUNX2, OSX*), osteoblasts (*ALP, BMP2, COL1a1, BMP4, ONC*), and osteocytes (*OCN, OPN*) [36, 50]. The comparison of qRT-PCR results revealed that supplementation with EVs alongside differentiation media significantly enhanced the expression of osteogenic markers. Specifically, early osteogenic markers gradually increased from day 14, peaking at day 21. In contrast, EV

treatment groups demonstrated substantial increases in marker expression at earlier time points, with nearly a 100-fold enhancement compared to control groups. Similarly, CM supplemented with EVs showed an increased expression trend at day 14, with over a 50-fold increase, for late osteogenic markers such as *OPN*, the untreated DM groups displayed elevated expression at days 21 and 28. However, EV supplementation in both DM and CM groups resulted in approximately a 100-fold increase in OPN expression. These findings suggest that EVs can accelerate osteogenic differentiation and enhance bone repair or regeneration more effectively at earlier time points than differentiation media alone. A recent study showed that Osteo-EVs from hMSCs also upregulated osteogenic markers [51], suggesting MSC-derived EVs are promising for bone tissue engineering and regenerative medicine, especially where traditional chemical inducers are limited or undesirable.

Our study showed that rBMSC-derived EVs play in osteogenic differentiation, even in the absence of traditional chemical stimuli such as L-ascorbic acid, dexamethasone, and β-glycerophosphate. This finding is particularly significant as it highlights the inherent osteogenic potential of these EVs in a chemically neutral environment. Given that the differentiation was less pronounced than DM-treated cells, increasing concentrations of EVs were tested, reaching up to 100 μg/ml in the CM group over a 14-day days to validate this effect. The results demonstrated a concentration-dependent increase in calcium deposition, suggesting that higher concentrations of rBMSC-derived EVs enhance osteogenic activity. Specifically, lower concentrations (12.5, 25, and 50 μg/ml) yielded minimal calcium deposits, whereas higher concentrations (75 and 100 μg/ml) led to substantial calcium deposition, as confirmed by ARS staining. We used FBS-EVs as a control to confirm that this enhanced osteogenic induction is specific to EVs derived from rBMCS rather than a general effect of any EVs. The significantly higher calcium deposition observed in groups treated with rBMSC-derived EVs than those treated with FBS-EVs indicates that the osteogenic potential of rBMSC-derived EVs is due to their unique composition rather than mere presence. FBS-EVs showed only a slight increase in calcium deposition, highlighting the superior osteogenic capacity of rBMSC-derived EVs. The enhanced osteogenic differentiation associated with rBMSC-derived EVs is likely due to specific proteins, lipids, or RNAs within these vesicles that promote osteogenic signaling pathways.

The ability to induce osteogenic differentiation using rBMSC-derived EVs without chemical agents could simplify the process of bone regeneration therapies, reducing potential side effects associated with chemical inducers. Additionally, the use of EVs offers a cell-free therapeutic approach, which can overcome some of the limitations and ethical concerns related to stem cell transplantation [52]. The demonstrated concentration-dependent effect of rBMSC-derived EVs on calcium deposition also provides a foundation for optimizing EV concentrations in therapeutic applications, ensuring maximal osteogenic outcomes.

Research has shown that EVs can carry a variety of bioactive molecules, including miRNAs and growth factors, which are essential for cell communication and differentiation. [53]. EVs have been found to carry proteins like BMPs, which are crucial for bone formation and regeneration [54]. Recent studies show that EVs derived from MSCs can promote osteogenesis by activating essential signaling pathways

such as Wnt/β-catenin and PI3K/Akt, crucial for bone formation and homeostasis. [55]. The observed upregulation of osteogenic markers such as *RUNX2, ALP, and OCN* in cells treated with MSC-derived EVs further supports their potential as osteoinductive agents [56]. The findings have significant implications for regenerative medicine, especially in bone tissue engineering and repair. The ability to induce osteogenic differentiation using EVs derived from rBMSCs without chemical inducers could streamline bone regeneration therapies, minimizing potential side effects associated with chemical agents. Moreover, EVs provide a cell-free therapeutic option, addressing some limitations and ethical concerns associated with stem cell transplantation [52].

Future investigations should focus on understanding the specific molecular mechanisms through which rBMSC-derived EVs promote osteogenic differentiation, including detailed analysis of their miRNA, protein, and lipid cargo. Mass spectrometry analysis will identify key factors and proteins involved in bone regeneration. Additionally, exploring the combination of EVs with other regenerative strategies, such as biomaterials and gene editing, may enhance the effectiveness of bone regeneration therapies. In vivo studies are crucial for evaluating the functional outcomes of EVs in bone healing and repair, whereas clinical trials will be needed to verify the safety and efficacy of rBMSC-derived EVs in human patients, potentially leading to their integration into established protocols for bone repair and regeneration.

CONCLUSION

This study has systematically optimized methods for producing high-purity EVs specifically tailored for bone regeneration. The findings demonstrate that these EVs alone can effectively stimulate osteogenic differentiation in vitro, establishing rBMSC-derived EVs as a significant advancement in bone tissue engineering. Key aspects of the research, including the identification of optimal source cells, refinement of EV isolation techniques, and evaluation of EVs' capacity to enhance osteogenic differentiation in progenitor cells, have been thoroughly investigated and conclusions supported by robust data. The methodologies developed here in can be used with human autologous cells in clinical applications related to bone tissue engineering. Leveraging these refined techniques will enable the bio-manufacture of bone-specific EVs that can be integrated into an appropriate biomaterial matrix. This results in a composite product designed for localized application in areas of bone defects. Such an innovative approach offers significant potential to enhance bone tissue regeneration, thereby facilitating faster recovery for patients suffering from bone defects.

Declarations

CONFLICTS OF INTEREST

The authors state that the research was carried out without any commercial or financial relationships that might be perceived as potential conflicts of interest.

ETHICS APPROVAL

The research conducted in this study received ethical approval from the Institutional Animal Ethics Committee of SCTIMST, under the approval number SCT/IAEC/TR-02/116/AUG/2023. This ensures that all animal experimentation adheres to ethical guidelines and regulations, prioritizing animal welfare.

CONSENT TO PARTICIPATE

Not applicable

CONSENT FOR PUBLICATION

All authors have reviewed and given their approval for this publication.

FUNDING INFORMATION

This work was supported by the Department of Biotechnology, Government of India (DBT-ATGC No. BT/PR42432/ATGC/127/135/2022).

Author Contribution

GA-Conceptualization, Data Curation, Methodology, Writing- Original draft. SG- Supervision, Resources, Writing- review, and editing. MU-Conceptualization, Formal analysis, Resources, Supervision, Validation, Writing- review and editing. MK-Supervision, Funding acquisition, Writing- review and editing. The final version of the manuscript was reviewed and approved by all authors.

Acknowledgement

The authors thank Dr. Rekha MR, Dr. Anil Kumar PR, and Joseph Xavier from SCTIMST for supporting DLS, Cell culture studies, and flow cytometry evaluations. The authors thank Dr. Cibin TR and Aishwarya Babu from SCTIMST for their valuable suggestions and assistance.

AVAILABILITY OF DATA AND MATERIAL

All data from this study can be found in the publication and its supplementary materials. Additional resources utilized in this research can be obtained from the corresponding authors upon request.

References

1. Lee KS et al (Oct. 2021) Extracellular vesicles from adipose tissue-derived stem cells alleviate osteoporosis through osteoprotegerin and *miR-21-5*. J Extracell Vesicles 10(12):e12152.

10.1002/jev2.12152

2. Kuang M et al (2019) Exosomes derived from Wharton's jelly of human umbilical cord mesenchymal stem cells reduce osteocyte apoptosis in glucocorticoid-induced osteonecrosis of the femoral head in rats via the miR-21-PTEN-AKT signalling pathway. Int J Biol Sci 15(9):1861–1871. 10.7150/ijbs.32262
3. Lu G, Cheng P, Liu T, Wang Z (Dec. 2020) Exosomal miR-29a Promotes Angiogenesis and Osteogenesis. Front Cell Dev Biol 8:608521. 10.3389/fcell.2020.608521
4. Li X, Zhang Y, Qi G (May 2013) Evaluation of isolation methods and culture conditions for rat bone marrow mesenchymal stem cells. Cytotechnology 65(3):323–334. 10.1007/s10616-012-9497-3
5. Pittenger MF et al (1999) Apr., Multilineage potential of adult human mesenchymal stem cells, *Science*, vol. 284, no. 5411, pp. 143–147. 10.1126/science.284.5411.143
6. Riazifar M, Pone EJ, Lötvall J, Zhao W (Jan. 2017) Stem Cell Extracellular Vesicles: Extended Messages of Regeneration. Annu Rev Pharmacol Toxicol 57(1):125–154. 10.1146/annurev-pharmtox-061616-030146
7. Liu A et al (May 2021) Optimized BMSC-derived osteoinductive exosomes immobilized in hierarchical scaffold via lyophilization for bone repair through Bmpr2/Acvr2b competitive receptor-activated Smad pathway. Biomaterials 272:120718. 10.1016/j.biomaterials.2021.120718
8. Zaborowski MP, Balaj L, Breakefield XO, Lai CP (2015) Extracellular Vesicles: Composition, Biological Relevance, and Methods of Study, *Bioscience*, vol. 65, no. 8, pp. 783–797, Aug. 10.1093/biosci/biv084
9. Doyle LM, Wang MZ (2019) Overview of Extracellular Vesicles, Their Origin, Composition, Purpose, and Methods for Exosome Isolation and Analysis, *Cells*, vol. 8, no. 7, p. 727, Jul. 10.3390/cells8070727
10. Kumar MA et al (Feb. 2024) Extracellular vesicles as tools and targets in therapy for diseases. Signal Transduct Target Ther 9(1):1–41. 10.1038/s41392-024-01735-1
11. Jiao Y et al (Jan. 2024) Advances in the Study of Extracellular Vesicles for Bone Regeneration. Int J Mol Sci 25 6, Art. 6. 10.3390/ijms25063480
12. Maiti SK (Oct. 2017) Mesenchymal Stem Cells Derived from Rat Bone Marrow (rBM MSC): Techniques for Isolation, Expansion and Differentiation. J Stem Cell Res Ther 3(3). 10.15406/jsrt.2017.03.00101
13. Shami-shah A, Travis BG, Walt DR (2023) Advances in extracellular vesicle isolation methods: a path towards cell-type specific EV isolation, *Extracell. Vesicles Circ. Nucleic Acids*, vol. 4, no. 3, pp. 447–460, Jul. 10.20517/evcna.2023.14
14. Guerreiro EM et al (Sep. 2018) Efficient extracellular vesicle isolation by combining cell media modifications, ultrafiltration, and size-exclusion chromatography. PLoS ONE 13(9):e0204276. 10.1371/journal.pone.0204276
15. Rufo J et al (Feb. 2024) High-yield and rapid isolation of extracellular vesicles by flocculation via orbital acoustic trapping: FLOAT. Microsyst Nanoeng 10(1):23. 10.1038/s41378-023-00648-3

16. Gorgzadeh A et al (Jan. 2024) A state-of-the-art review of the recent advances in exosome isolation and detection methods in viral infection. Virol J 21(1):34. 10.1186/s12985-024-02301-5
17. Omrani M et al (2024) Mar., Global trend in exosome isolation and application: an update concept in management of diseases, *Mol. Cell. Biochem.*, vol. 479, no. 3, pp. 679–691. 10.1007/s11010-023-04756-6
18. Sharif S et al (2007) Mar., The potential use of bone marrow stromal cells for cochlear cell therapy, *Neuroreport*, vol. 18, no. 4, pp. 351–354. 10.1097/WNR.0b013e3280287a9a
19. Huang S, Xu L, Sun Y, Wu T, Wang K, Li G (Jan. 2015) An improved protocol for isolation and culture of mesenchymal stem cells from mouse bone marrow. J Orthop Transl 3(1):26–33. 10.1016/j.jot.2014.07.005
20. Ar N, Maiti SK, Mu SK, Kumar S, Saxena A, Kumar N (2017) Isolation, proliferation, characterization and in vivo osteogenic potential of bone- marrow derived mesenchymal stem cells (rBMSC) in rabbit model. INDIAN J EXP BIOL
21. Kacham S et al (May 2021) Human Umbilical Cord-Derived Mesenchymal Stem Cells Promote Corneal Epithelial Repair In Vitro. Cells 10(5):1254. 10.3390/cells10051254
22. Cho S-R et al (2009) Dec., Functional Recovery after the Transplantation of Neurally Differentiated Mesenchymal Stem Cells Derived from Bone Barrow in a Rat Model of Spinal Cord Injury, *Cell Transplant.*, vol. 18, no. 12, pp. 1359–1368. 10.3727/096368909X475329
23. Le Gall L et al (Jul. 2020) Optimized method for extraction of exosomes from human primary muscle cells. Skelet Muscle 10(1). 10.1186/s13395-020-00238-1
24. Rider MA, Hurwitz SN, Meckes DG (2016) ExtraPEG: A Polyethylene Glycol-Based Method for Enrichment of Extracellular Vesicles, *Sci. Rep.*, vol. 6, no. 1, Art. no. 1, Apr. 10.1038/srep23978
25. Théry C, Amigorena S, Raposo G, Clayton A (Mar. 2006) Isolation and Characterization of Exosomes from Cell Culture Supernatants and Biological Fluids. Curr Protoc Cell Biol 30(1). 10.1002/0471143030.cb0322s30
26. Jang M et al (Dec. 2019) Extracellular vesicle (EV)-polyphenol nanoaggregates for microRNA-based cancer diagnosis. NPG Asia Mater 11(1):79. 10.1038/s41427-019-0184-0
27. Soares Martins T, Catita J, Martins Rosa I, O. A. B. da Cruz e Silva, and, Henriques AG (2018) Exosome isolation from distinct biofluids using precipitation and column-based approaches, *PLOS ONE*, vol. 13, no. 6, p. e0198820, Jun. 10.1371/journal.pone.0198820
28. Shelke GV, Lässer C, Gho YS, Lötvall J (2014) Sep., Importance of exosome depletion protocols to eliminate functional and RNA-containing extracellular vesicles from fetal bovine serum, *J. Extracell. Vesicles*, vol. 3, p. 10.3402/jev.v3.24783, doi: 10.3402/jev.v3.24783
29. Eitan E, Zhang S, Witwer KW, Mattson MP (Jan. 2015) Extracellular vesicle–depleted fetal bovine and human sera have reduced capacity to support cell growth. J Extracell Vesicles 4(1):26373. 10.3402/jev.v4.26373
30. Mollentze J, Durandt C, Pepper MS (2021) An In Vitro and In Vivo Comparison of Osteogenic Differentiation of Human Mesenchymal Stromal/Stem Cells, *Stem Cells Int.*, vol. pp. 1–23, Sep.

2021. 10.1155/2021/9919361

31. Meesuk L et al (Nov. 2022) Osteogenic differentiation and proliferation potentials of human bone marrow and umbilical cord-derived mesenchymal stem cells on the 3D-printed hydroxyapatite scaffolds. Sci Rep 12(1):19509. 10.1038/s41598-022-24160-2
32. López-González I, Zamora-Ledezma C, Sanchez-Lorencio MI, Tristante Barrenechea E, Gabaldón-Hernández JA, Meseguer-Olmo L (2021) Modifications in Gene Expression in the Process of Osteoblastic Differentiation of Multipotent Bone Marrow-Derived Human Mesenchymal Stem Cells Induced by a Novel Osteoinductive Porous Medical-Grade 3D-Printed Poly(ε-caprolactone)/β-tricalcium Phosphate Composite, *Int. J. Mol. Sci.*, vol. 22, no. 20, p. 11216, Oct. 10.3390/ijms222011216
33. Mi L et al (Apr. 2022) The Mechanism of Stem Cell Aging. Stem Cell Rev Rep 18(4):1281–1293. 10.1007/s12015-021-10317-5
34. Larijani B et al (2021) Opportunities and Challenges in Stem Cell Aging. in Cell Biology and Translational Medicine, Volume 13. Springer, Cham, pp 143–175. doi: 10.1007/5584_2021_624.
35. Yang J-D, Cheng-Huang J-C, Wang X-M, Feng Y-N, Li, Xiao H-X (Dec. 2014) The isolation and cultivation of bone marrow stem cells and evaluation of differences for neural-like cells differentiation under the induction with neurotrophic factors. Cytotechnology 66(6):1007–1019. 10.1007/s10616-013-9654-3
36. Patel GK et al (Dec. 2019) Comparative analysis of exosome isolation methods using culture supernatant for optimum yield, purity and downstream applications. Sci Rep 9(1):5335. 10.1038/s41598-019-41800-2
37. Lee Y, Ni J, Wasinger VC, Graham P, Li Y (2023) Comparison Study of Small Extracellular Vesicle Isolation Methods for Profiling Protein Biomarkers in Breast Cancer Liquid Biopsies. Int J Mol Sci 24 20, Art. 20, Jan. 10.3390/ijms242015462
38. Zheng Y et al (2023) Apr., Production and Biological Effects of Extracellular Vesicles from Adipose-Derived Stem Cells Were Markedly Increased by Low-Intensity Ultrasound Stimulation for Promoting Diabetic Wound Healing, *Stem Cell Rev. Rep.*, vol. 19, no. 3, pp. 784–806. 10.1007/s12015-022-10487-w
39. Mulcahy LA, Pink RC, Carter DRF (Jan. 2014) Routes and mechanisms of extracellular vesicle uptake. J Extracell Vesicles 3(1):24641. 10.3402/jev.v3.24641
40. Cha JM et al (Jan. 2018) Efficient scalable production of therapeutic microvesicles derived from human mesenchymal stem cells. Sci Rep 8(1):1171. 10.1038/s41598-018-19211-6
41. Jang SC et al (2013) Sep., Bioinspired Exosome-Mimetic Nanovesicles for Targeted Delivery of Chemotherapeutics to Malignant Tumors, *ACS Nano*, vol. 7, no. 9, pp. 7698–7710. 10.1021/nn402232g
42. Wang H, Yang Z, Ai S, Xiao J (2023) Updated Methods of Extracellular Vesicles Isolation. In: Xiao J (ed) in Extracellular Vesicles in Cardiovascular and Metabolic Diseases. Singapore: Springer Nature, pp 3–14. doi: 10.1007/978-981-99-1443-2_1.

43. Li J et al (May 2015) Serum-free culture alters the quantity and protein composition of neuroblastoma-derived extracellular vesicles. J Extracell Vesicles 4. 10.3402/jev.v4.26883
44. Lehrich BM, Liang Y, Fiandaca MS (Jan. 2021) Foetal bovine serum influence on in vitro extracellular vesicle analyses. J Extracell Vesicles 10(3):e12061. 10.1002/jev2.12061
45. Zhang X et al (Mar. 2023) Osteoblast derived extracellular vesicles induced by dexamethasone: A novel biomimetic tool for enhancing osteogenesis in vitro. Front Bioeng Biotechnol 11:1160703. 10.3389/fbioe.2023.1160703
46. Neves Boeloni J, Melo Ocarino N, Miranda Goes A, Serakides R (2014) Comparative study of osteogenic differentiation potential of mesenchymal stem cells derived from bone marrow and adipose tissue of osteoporotic female rats, *Connect. Tissue Res.*, vol. 55, no. 2, pp. 103–114, Apr. 10.3109/03008207.2013.860970
47. Taghdiri Nooshabadi V et al (2019) Sep., Endometrial Mesenchymal Stem Cell-Derived Exosome Promote Endothelial Cell Angiogenesis in a Dose Dependent Manner: A New Perspective on Regenerative Medicine and Cell-Free Therapy, *Arch. Neurosci.*, vol. 6, no. 4. 10.5812/ans.94041
48. Go Y-Y, Lee C-M, Chae S-W, Song J-J (Sep. 2022) Osteogenic Efficacy of Human Trophoblasts-Derived Conditioned Medium on Mesenchymal Stem Cells. Int J Mol Sci 23(17):10196. 10.3390/ijms231710196
49. Wang X, Omar O, Vazirisani F, Thomsen P, Ekström K (Feb. 2018) Mesenchymal stem cell-derived exosomes have altered microRNA profiles and induce osteogenic differentiation depending on the stage of differentiation. PLoS ONE 13(2):e0193059. 10.1371/journal.pone.0193059
50. Toupadakis CA et al (2010) Comparison of the osteogenic potential of equine mesenchymal stem cells from bone marrow, adipose tissue, umbilical cord blood, and umbilical cord tissue. Oct. 10.2460/ajvr.71.10.1237
51. Al-Sharabi N et al (Feb. 2024) Osteogenic human MSC-derived extracellular vesicles regulate MSC activity and osteogenic differentiation and promote bone regeneration in a rat calvarial defect model. Stem Cell Res Ther 15(1):33. 10.1186/s13287-024-03639-x
52. Lai H, Li J, Kou X, Mao X, Zhao W, Ma L (2023) Extracellular Vesicles for Dental Pulp and Periodontal Regeneration, *Pharmaceutics*, vol. 15, no. 1, p. 282, Jan. 10.3390/pharmaceutics15010282
53. Kalluri R, LeBleu VS (Feb. 2020) The biology, function, and biomedical applications of exosomes. Science 367:eaau6977. no. 647810.1126/science.aau6977
54. Davies OG (May 2023) Extracellular vesicles: From bone development to regenerative orthopedics. Mol Ther 31(5):1251–1274. 10.1016/j.ymthe.2023.02.021
55. Fuloria S et al (Feb. 2021) Mesenchymal Stem Cell-Derived Extracellular Vesicles: Regenerative Potential and Challenges. Biology 10(3):172. 10.3390/biology10030172
56. Tsiapalis D, O'Driscoll L (Apr. 2020) Mesenchymal Stem Cell Derived Extracellular Vesicles for Tissue Engineering and Regenerative Medicine Applications. Cells 9(4):991. 10.3390/cells9040991

Figures

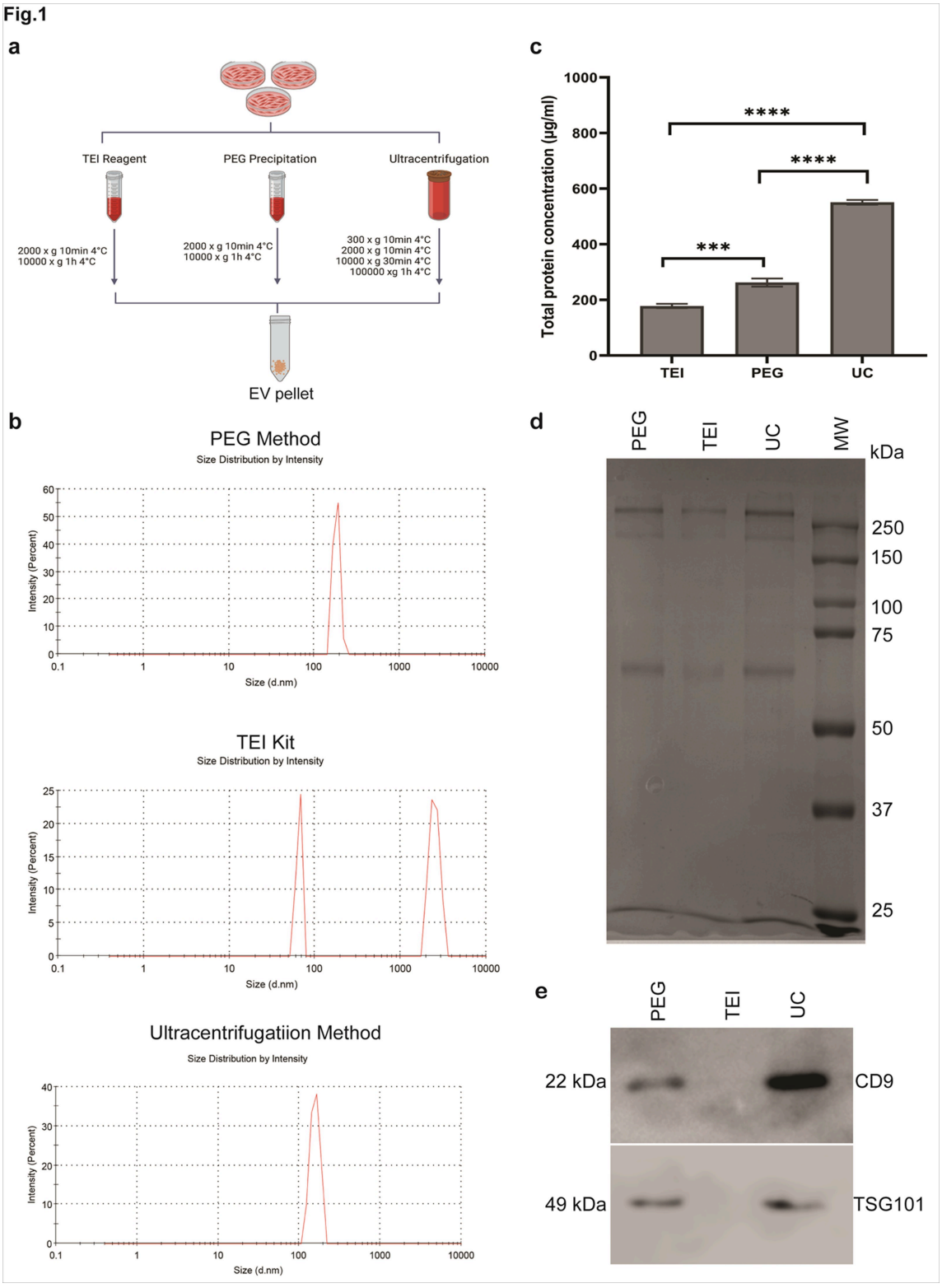

Figure 1

Evaluation of EV Isolation Methods. (a) Schematic of the experimental of EV isolation methods: TEI, PEG precipitation, and UC **(b)**Size distribution of EVs measured by DLS. The experiments were conducted in triplicate, with results presented as mean ± standard deviation. **(c)** The total EV yield was quantified using BCA assay kit. **(d)** Protein bands in EVs isolated via UC, PEG precipitation, and TEI kit methods were visualized using SDS-PAGE analysis with Coomassie staining. **(e)** The western blot analyzed EV

markers CD9 and TSG101. The lanes correspond to 1- PEG method, 2- TEI Kit, and 3- Ultracentrifugation method. (MW-molecular weight marker). Statistical significance is denoted by ***P ≤ 0.001 and **** P ≤ 0.0001

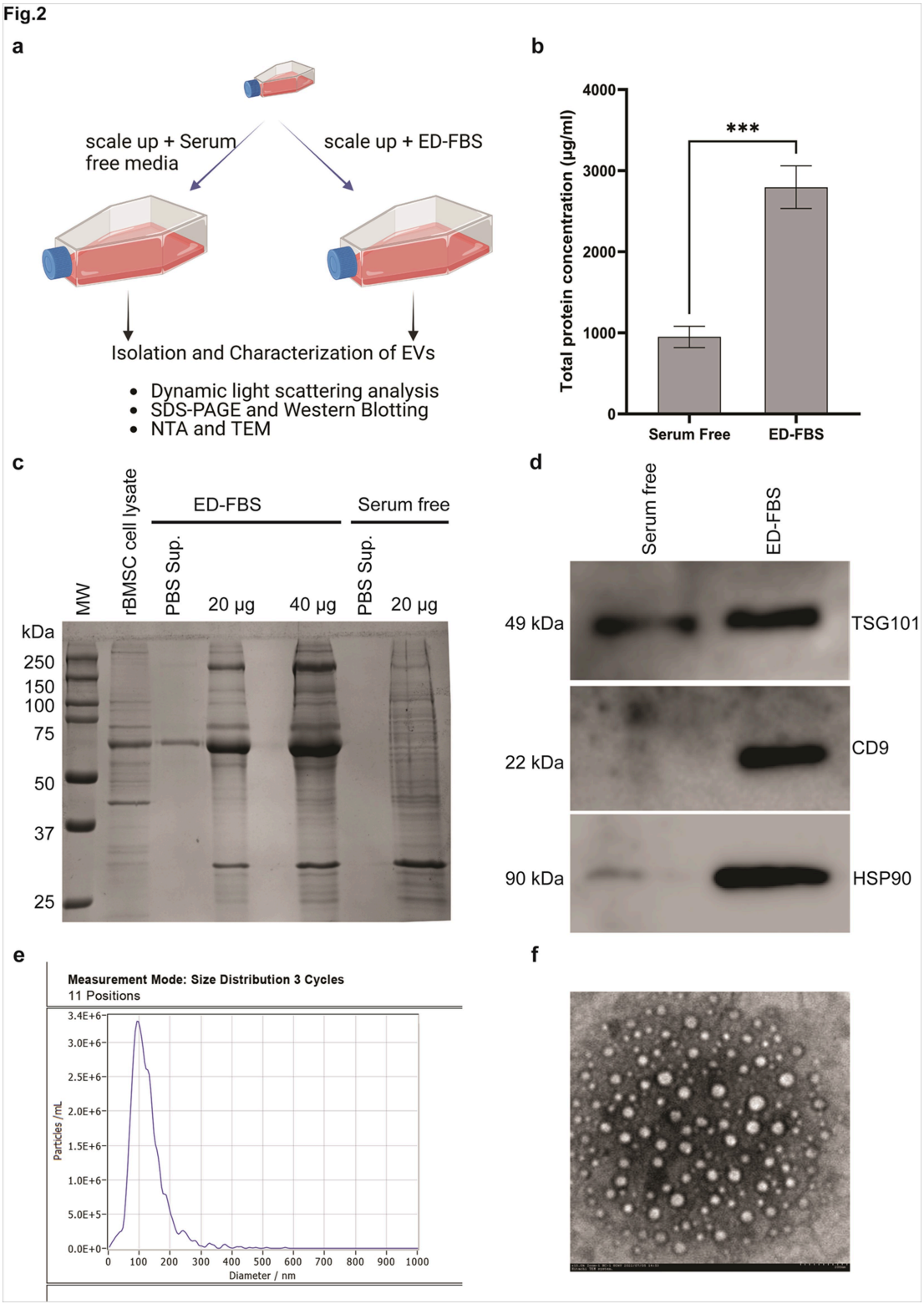

Figure 2

Methods to improve the exosomal yield. (a) Experimental workflow showing improved culture conditions. **(b)** Total protein estimation using BCA assay for EV samples isolated by supplementing ED-

FBS or serum-free media. **(c)** Protein profile was analyzed using SDS-PAGE and Coomassie blue staining. Lane 1 included MW, while Lane 2 had 15 µg of rBMSC lysate. Lanes 3 and 6 contained PBS supernatant obtained from EV isolation using the UC method. Lanes 4 and 5 were loaded with 20 µg and 40 µg of EV preparations derived from conditioned media supplemented with ED-FBS, while Lane 7 contained 20 µg of EV isolated from serum-free media using the UC method. **(d)** Western blot using primary antibodies for TSG101, HSP90, and CD9. **(e)** The size distribution of EVs was measured using NTA. **(f)** The Morphology of EVs was examined using TEM analysis (scale bar: 200nm). Statistical significance is indicated by *** $P \leq 0.001$

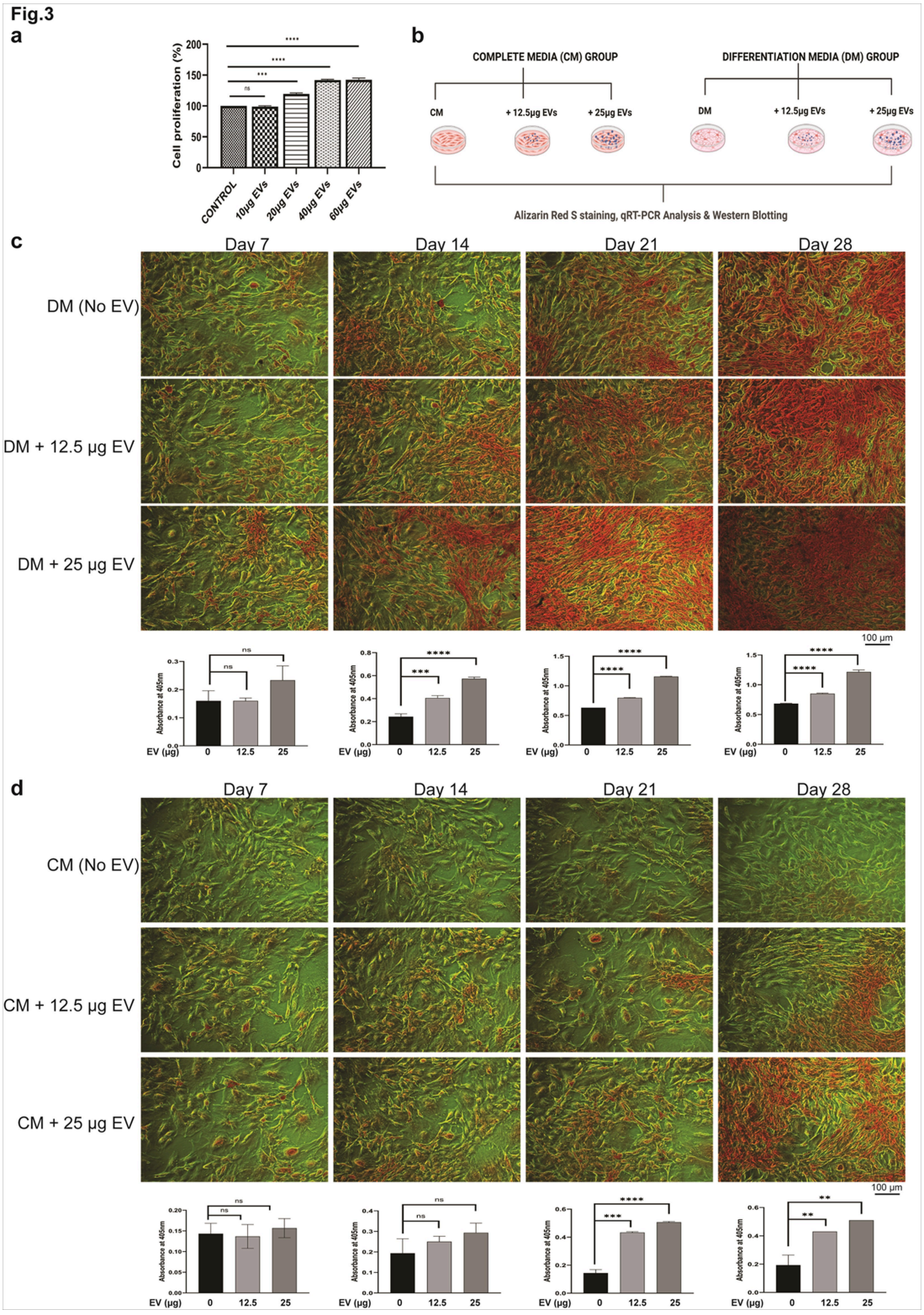

Figure 3

Effects of rBMSC-derived EVs on Osteogenic Differentiation and Cell Proliferation. (a) rBMSC-derived EVs were tested at concentrations of 12.5 and 25 µg, both in the presence and absence of osteogenic stimulants. **(b)** rBMSCs were treated with varying concentrations (0, 10, 20, 40, and 60 µg/ml) of EVs for 14 days, followed by MTT assay analysis. **(c)** Assessment of osteogenic differentiation through ARS staining. **(d)**Microscopic images of mineralization patterns (10x) of calcium deposition induced by EV

treatment (scale bars: 100 μm). Statistical significance indicated as ns P > 0.05, **P ≤ 0.01, ***P ≤ 0.001, and ****P ≤ 0.0001

Fig.4

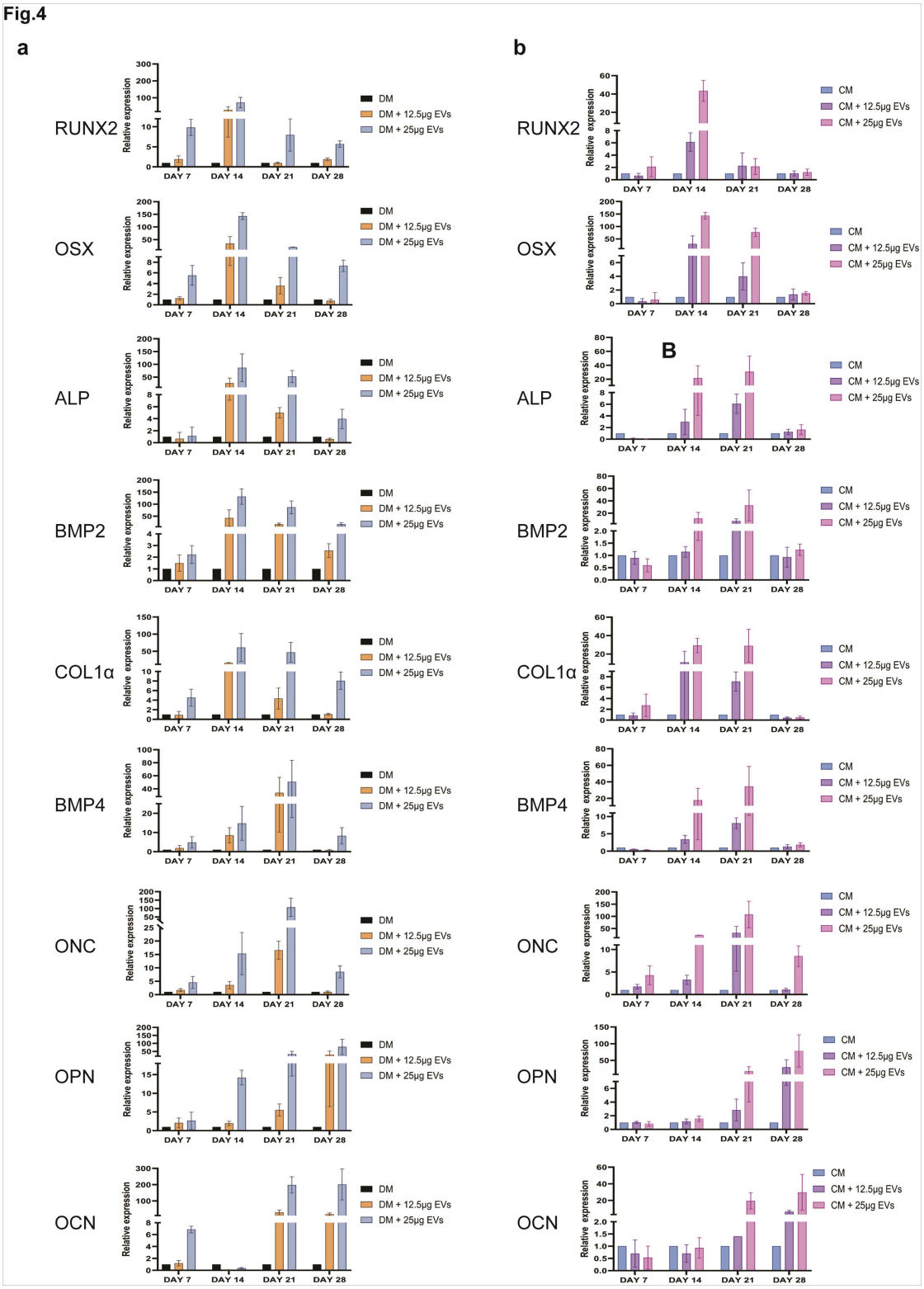

Figure 4

qRT-PCR analysis to confirm EV-enhanced osteogenic differentiation of rBMSCs. (a) qRT-PCR analysis of key osteogenic markers in rBMSCs treated with EVs under DM conditions at various time points (7, 14,

21, and 28 days) was performed using the ΔΔCt method. **(b)** Expression of osteogenic markers in the CM group treated with 25 μg/mL of EVs (CM + 25 μg EVs). Protein expression was normalized to β-Actin

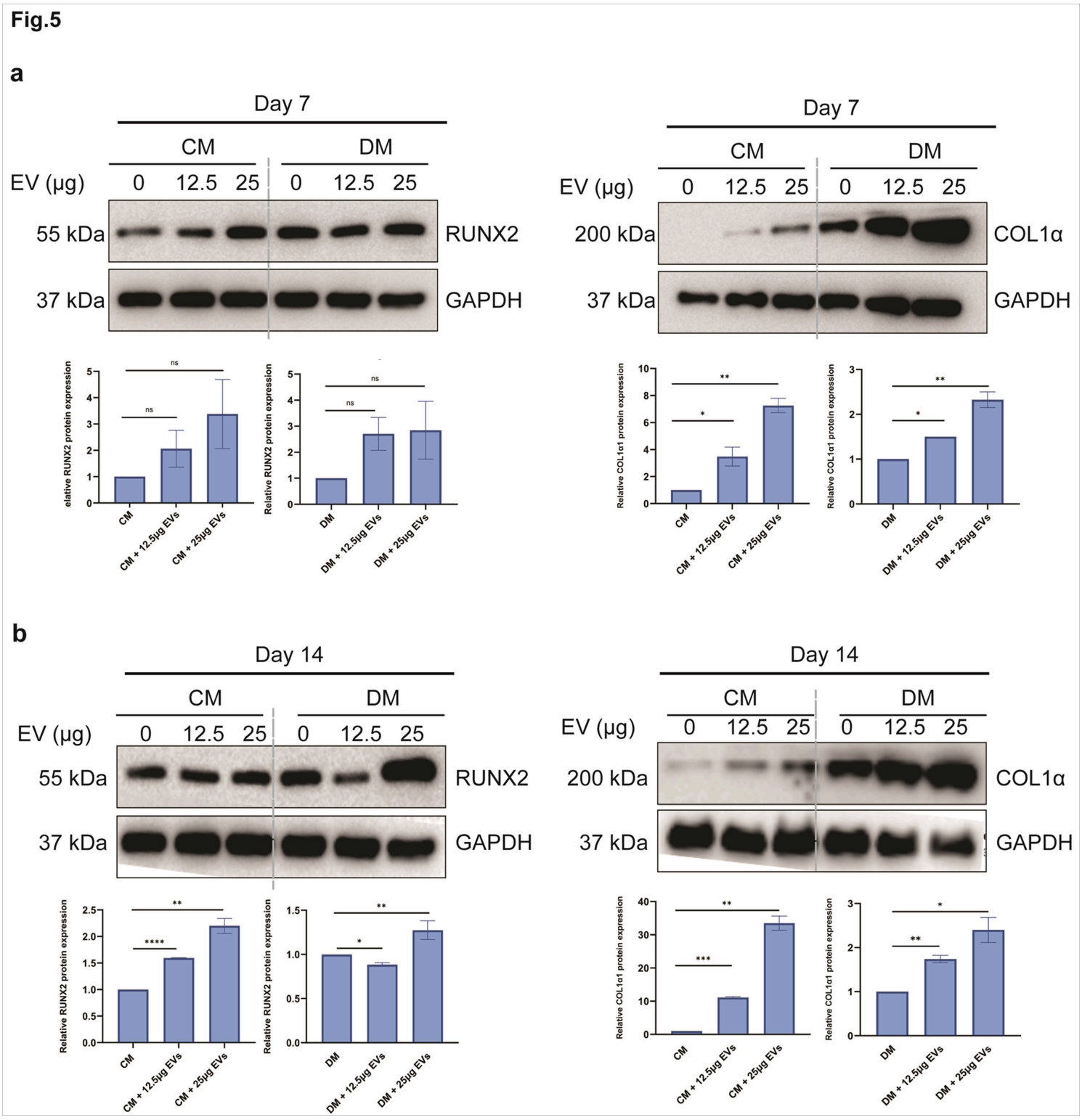

Figure 5

Protein Expression Analysis of RUNX2 and COL1α1 in rBMSCs Treated with EVs under CM and DM Conditions. Western blot analysis, preceded by SDS-PAGE, was conducted using specific primary antibodies: Anti-RUNX2, Anti-COL1α1, and Anti-GAPDH.**(a)** RUNX2 and **(b)** COL1α1 expression in rBMSCs

treated with EVs under CM and DM conditions were similarly examined through Western blot. ImageJ software was used to perform a comparative analysis of gray values for relevant protein bands. Statistical significance indicated as ns P > 0.05, **P ≤ 0.01, ***P ≤ 0.001, and ****P ≤ 0.0001

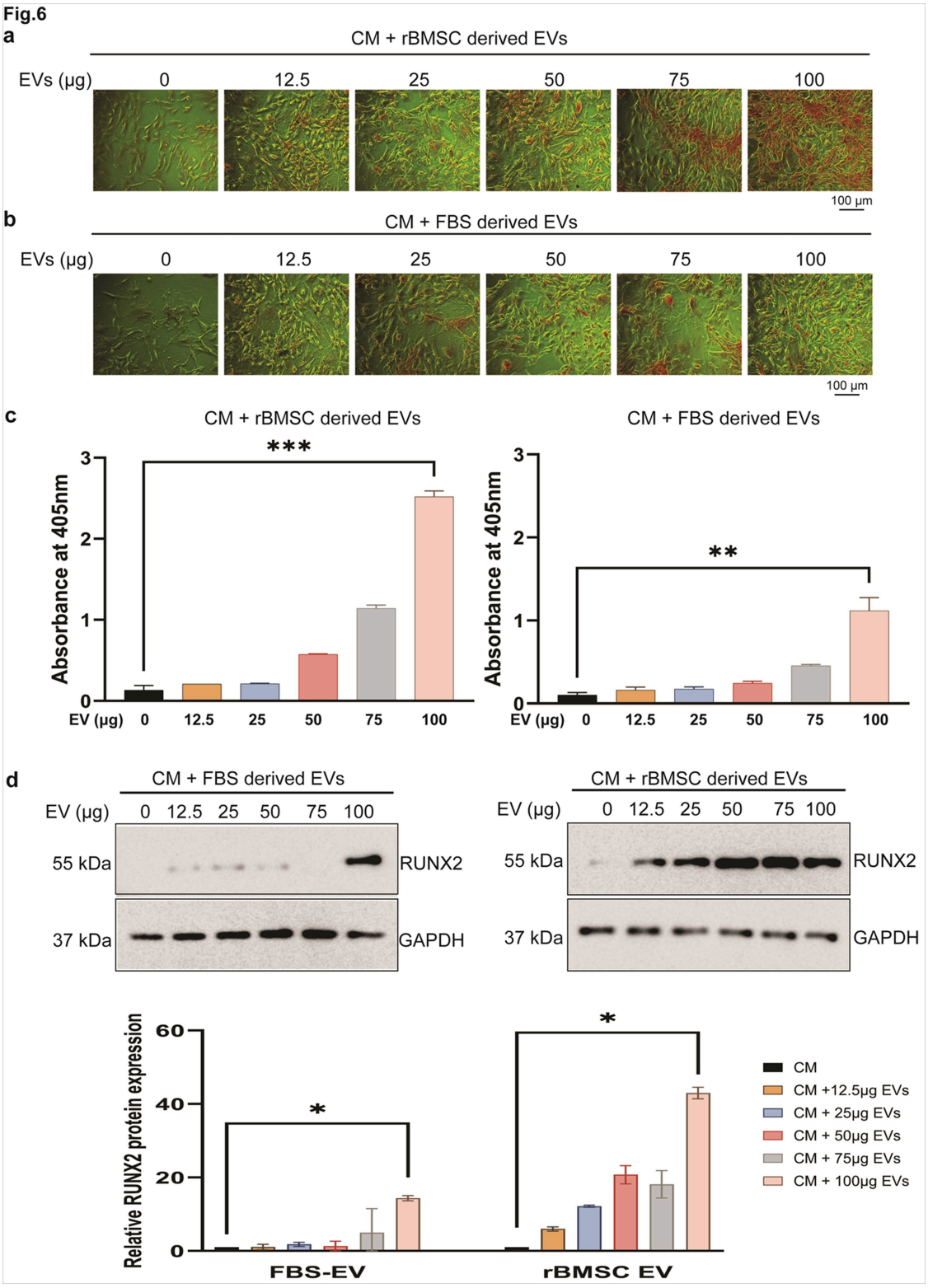

Figure 6

Enhanced osteogenic differentiation by rBMSC-Derived EVs. (a) ARS staining images depicting calcium deposition in rBMSCs grown in complete media and treated for 14 days (12.5, 25, 50, 75, and 100 μg/ml)

with rBMSC-derived EVs and **(b)**FBS-EVs. **(c)** Calcium deposition was quantified and expressed relative to the untreated control. **(d)** Western blot analysis of RUNX2 expression in rBMCs on treatment with FBS-EVs and rBMSC-derived EVs with varying concentrations. Comparative analysis of gray values for relevant protein bands using ImageJ software. Statistical significance is marked by **p < 0.01 and *p < 0.001

Supplementary Files

This is a list of supplementary files associated with this preprint. Click to download.

- SupplementaryData.docx